

# CAN VISUAL INPUT BE COMPRESSED? A VISUAL INPUT TOKEN COMPRESSION BENCHMARK FOR LARGE MULTIMODAL MODELS

006 **Anonymous authors**

007 Paper under double-blind review

## ABSTRACT

013 Large multimodal models (LMMs) often suffer from severe inference inefficiency  
 014 due to the large number of visual tokens introduced by image encoders. While  
 015 recent token compression methods, such as pruning and merging, have shown  
 016 promise in reducing redundancy, their evaluation remains fragmented and incon-  
 017 sistent. In this work, we present **UniPruneBench**, a unified and extensible bench-  
 018 mark for visual token pruning in multimodal LLMs. UniPruneBench provides  
 019 standardized protocols across six ability dimensions and ten datasets, covering ten  
 020 representative compression algorithms and three families of LMMs (LLaVA-v1.5,  
 021 Intern-VL3, and Qwen2.5-VL). Beyond task accuracy, it incorporates system-  
 022 level metrics such as runtime and prefilling latency to provide a holistic view.  
 023 Our experiments uncover several key findings: (1) random pruning is a surpris-  
 024 ingly strong baseline, (2) no single method consistently outperforms others across  
 025 scenarios, (3) pruning sensitivity varies significantly across tasks, with OCR be-  
 026 ing most vulnerable, and (4) pruning ratio is the dominant factor governing perfor-  
 027 mance degradation. We believe UniPruneBench will serve as a reliable foundation  
 028 for future research on efficient multimodal modeling.

## 1 INTRODUCTION

031 Recently, large multimodal models (LMMs) have achieved remarkable progress across a wide range  
 032 of multimodal tasks. These models are typically built upon pre-trained large language models  
 033 (LLMs) by integrating visual encoders (e.g., CLIP (Radford et al., 2021), CoCa (Yu et al., 2022)) and  
 034 lightweight adapter modules. The visual encoders transform images into sequences of visual tokens,  
 035 while the adapters bridge these visual representations with the textual space, enabling seamless mul-  
 036 timodal understanding and reasoning. Representative LMMs follow two main adapter paradigms:  
 037 BLIP-style models that rely on cross-modal attention and LLaVA-style models that concatenate ViT  
 038 patch tokens into the LLM context with MLP layers. These approaches, exemplified by LLaVA (Liu  
 039 et al., 2023a), Qwen-VL (Yang et al., 2024), and Intern-VL (Zhu et al., 2025), have achieved strong  
 040 performance in visual question answering (VQA), grounding, and multimodal reasoning.

041 However, incorporating visual inputs into LMMs inevitably introduces a large number of visual  
 042 tokens, leading to substantial redundancy and creating a strong demand for faster inference (Vasu  
 043 et al., 2025; Wen et al., 2025a). Unlike text tokens, which are semantically dense, visual tokens are  
 044 often redundant and highly correlated (Bi et al., 2025b). Directly appending hundreds of tokens per  
 045 image leads to steep increases in computation, memory usage, and inference latency, posing severe  
 046 bottlenecks for real-time and large-scale deployment. Moreover, for many vision-language tasks  
 047 such as VQA, it is unnecessary to process the entire image. Only a subset of task-relevant regions  
 048 needs to be considered, further highlighting the inefficiency of uniform dense tokenization.

049 To address this, visual token compression has emerged as a promising direction. Recent work ex-  
 050 plores token pruning and merging to reduce redundancy while preserving essential semantics. For  
 051 example, FastV (Vasu et al., 2025) prunes tokens with low attention scores, PyramidDrop (Xing  
 052 et al., 2024) shrinks sequences in a layer-wise schedule, AdaptInfer (Zhang et al., 2025a) uses a  
 053 dynamic text-guided mechanism to reuse hierarchical text-to-text attention maps to construct a soft  
 prior for token importance, Recoverable Compression (Chen et al., 2025) restores filtered key tokens

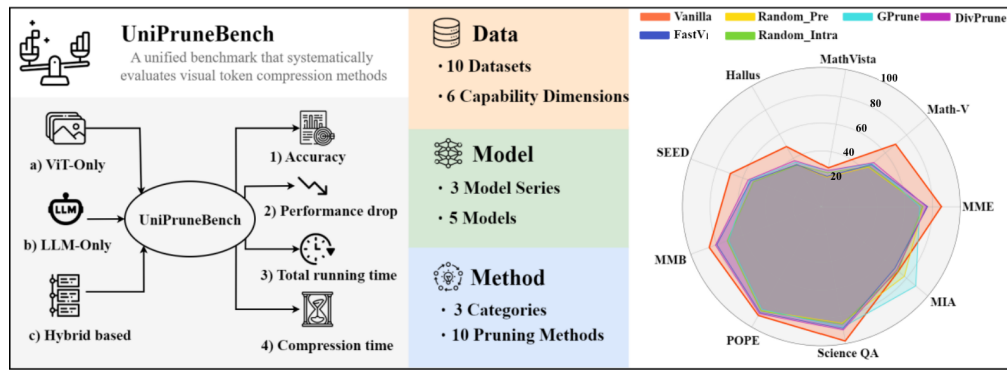


Figure 1: Overview of UniPruneBench, along with experimental results for representative pruning methods across various data scenarios.

related to the text based on text-visual similarity, DCP (Jiang et al., 2025a) selects key tokens related to the text through a text-aware computation module and preserves visual structural information through an image-aware computation module, HoloV (Zou et al., 2025) generates a composite score by combining intra-modal semantic diversity with visual attention saliency, and GridPrune (Duan et al., 2025) dynamically allocates token budgets to image grid regions based on text-conditioned correlation. Such methods reduce computation and memory and are compatible with existing LMMs due to their ability to process variable-length inputs.

Despite these advances, existing token compression methods lack a fair and systematic evaluation: **1) Limited coverage of methods, model series, and downstream tasks:** Most prior work evaluates only a small subset of compression algorithms on a narrow set of datasets, preventing a comprehensive understanding across different downstream task scenarios. **2) Absence of standardized evaluation protocols:** Current studies adopt heterogeneous frameworks, such as LLaVA native eval, LMMS-Eval (Zhang et al., 2024), and VLMEvalKit (Duan et al., 2024b), with inconsistent prompt templates, scoring metrics, and token retention ratios. These inconsistencies make it difficult to reliably compare methods and reproduce reported results. **3) Neglect of system-level metrics and low modularity:** Evaluations typically focus on task accuracy while ignoring important metrics such as runtime and end-to-end latency. In addition, many pruning implementations are tightly coupled to specific architectures, limiting their flexibility and making it challenging to extend them to emerging multimodal models.

These limitations highlight the need for a **unified, extensible, and user-friendly benchmark** to enable fair and reproducible evaluation of token compression methods for multimodal LMMs. To achieve this, in this paper, we introduce the **Unified Visual Token Pruning Benchmark (UniPruneBench)**, a benchmark designed to systematically evaluate plug-and-play visual token compression algorithms. As shown in Fig 1, UniPruneBench is a standardized evaluation benchmark that offers a fair and unified platform for comparing visual token pruning techniques. In addition, it provides a modular and user-friendly interface that decouples pruning logic from model architecture, enabling seamless integration with various LMMs.

Specifically, UniPruneBench provides **(1)** a diverse and challenging benchmark spanning **six ability dimensions** (e.g., comprehensive understanding, OCR, mathematical reasoning, and hallucination) **across ten datasets**. **(2)** It categorizes existing plug-and-play token compression methods **into three types: ViT-only, LLM-only, and hybrid**, based on where token pruning is applied, and offers comprehensive evaluations of **ten representative algorithms**. Besides, **(3)** it conducts experiments on **three series of large multimodal models: LLaVA-v1.5, Intern-VL3, and Qwen2.5-VL**. In addition to measuring performance drop, **(4)** the benchmark also reports system-level metrics, **including total running time, prefilling time**, providing a holistic view of both accuracy and efficiency.

Through extensive experiments, UniPruneBench reveals key observations: **(1). Random pruning is a surprisingly strong baseline.** Despite its simplicity, random pruning often surpasses existing designed strategies, highlighting the need for stronger baselines; **(2). No single method dominates across scenarios.** Different methods excel under different models, pruning ratios, and datasets; **(3). Task sensitivity varies significantly.** Instruction-following tasks remain robust, while OCR benchmarks suffer the most severe degradation; **(4). Pruning ratio drives accuracy-efficiency**

108 **trade-offs.** Light pruning incurs only moderate drops, whereas aggressive pruning sharply degrades  
 109 performance; **(5). These trends are consistent across all three models, indicating generality.**  
 110

## 111 2 RELATED WORK

### 112 2.1 LARGE MULTIMODAL MODEL

113 Large Multimodal Models (LMMs) have brought significant breakthroughs in integrating vision and  
 114 language, enabling models to perform complex cross-modal understanding and reasoning tasks. A  
 115 typical end-to-end LMM consists of three major components: a language encoder, a vision encoder,  
 116 and a cross-modal interaction module (Caffagni et al., 2024). The language encoder is usually  
 117 adapted from large language models like LLaMA (Grattafiori et al., 2024; Touvron et al., 2023) and  
 118 Qwen (Yang et al., 2024), while the vision encoder often adopts architectures such as Vision Trans-  
 119 former (ViT) (Dosovitskiy et al., 2020). The cross-modality module connects the two modalities,  
 120 allowing language models to process visual inputs effectively.

121 Based on this architecture, various LMMs have been developed with different design choices and  
 122 training strategies. For instance, Qwen2.5-VL (Bai et al., 2025) introduces a visual receptor and  
 123 follows a structured multi-stage training process. Intern-VL3 (Chen et al., 2024b) adopts joint multi-  
 124 modal pretraining across large-scale datasets, while LLaVA (Liu et al., 2023a) and its successor  
 125 LLaVA-OneVision (Li et al., 2025) focus on enhancing visual grounding and reasoning through task-  
 126 aligned training with MLP layer. These approaches collectively push the limits of vision-language  
 127 alignment, leading to strong performance across a variety of multimodal benchmarks (Kil et al.,  
 128 2024; Huang & Zhang, 2024). In addition, recent work explores the use of LLM agents equipped  
 129 with visual tools (Gao et al., 2024; Fan et al., 2024; Gupta & Kembhavi, 2023; Bi et al., 2025c)  
 130 to handle more dynamic and interactive multimodal tasks. However, such agent-based methods go  
 131 beyond the scope of this paper, which focuses on the architectural and training advances of the agent  
 132 framework.

### 133 2.2 VISUAL TOKEN COMPRESSION BENCHMARK.

134 Few benchmarks have been proposed for this task. The most relevant prior analysis work proposed  
 135 in (Wen et al., 2025a), which evaluates only four token-pruning baselines, namely FastV, Sparse-  
 136 VLM, random, and pooling. And it does not provide source code or reproducible scripts. In contrast,  
 137 our work implements 10 state-of-the-art pruning algorithms and will release all implementation  
 138 details publicly. Moreover, we evaluate these methods across a wider range of downstream tasks and  
 139 metrics, providing a more comprehensive and reproducible benchmark.

## 140 3 UNIPRUNEBENCH

141 The UniPruneBench comprises six evaluation dimensions spanning ten datasets, each released under  
 142 permissive licenses that permit research use. In addition, it benchmarks ten representative methods  
 143 across three categories and covers five representative LMMs from three different model families.

### 144 3.1 VISUAL TOKEN COMPRESSION METHODS

145 LMM pruning aims to reduce redundant tokens while preserving model performance. Especially,  
 146 The number of visual tokens is usually tens to hundreds of times that of language tokens, and visual  
 147 signals are inherently more sparse, thus needing to be pruned. As shown in Fig 2, Existing plug-and-  
 148 play methods can be divided into three categories according to where to prune: **ViT-only method**  
 149 (Bolya et al., 2023; Jiang et al., 2025b), **LLM-only method** (Wen et al., 2025b; Ye et al., 2025),  
 150 and **Hybrid based method** (Zhang et al., 2025b; Liu et al., 2024a). Besides, one very basic method,  
 151 i.e., **random token pruning**, is also adopted as a strong baseline.

152 **ViT-only methods:** Token pruning in ViTs is achieved through two paradigms: token selection  
 153 and token merging. For token selection, **DivPrune** (Alvar et al., 2025) formulates pruning as a  
 154 subset selection problem that maximizes diversity, thus reducing redundancy while preserving rep-  
 155 resentative information. **G-Prune** (Jiang et al., 2025b) iteratively updates importance scores via  
 156 information propagation, retaining the most representative tokens from both foreground and back-  
 157

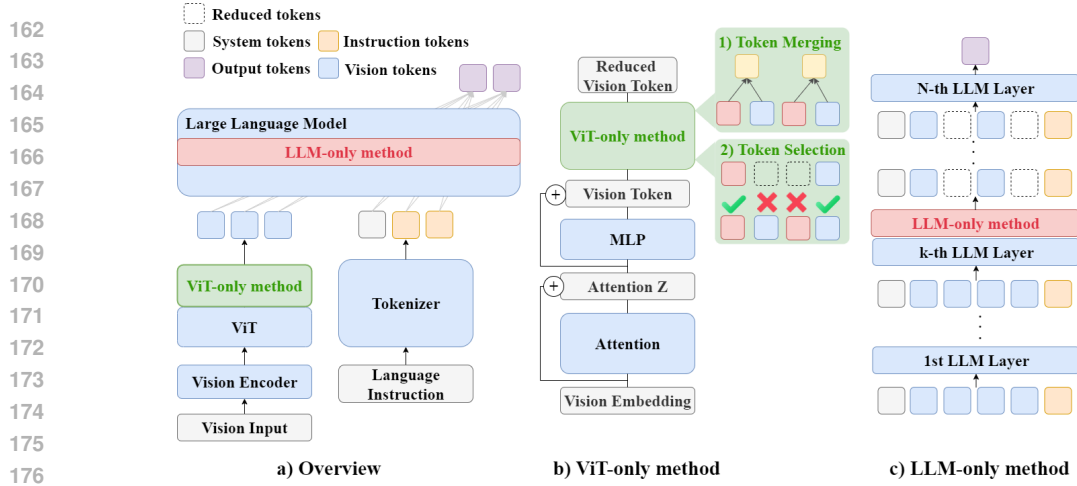


Figure 2: Taxonomy of visual token pruning Methods, including ViT-only, LLM-only, and hybrid. ground regions. **LLaVA-PruMerge** (Shang et al., 2024) further optimizes token processing in the CLIP image encoder through an adaptive token merging strategy.

**LLM-only methods:** These approaches prune visual tokens within the LLM to reduce computation while maintaining performance. **FastV** (Chen et al., 2024a) makes an early attempt by discarding tokens after the second layer of LMMs. **VTW** (Lin et al., 2025) argues that tokens can be entirely removed once the model reaches sufficient depth. **DART** (Wen et al., 2025b) selects a small set of pivot tokens and removes others with high redundancy.

**Hybrid methods:** Multi-stage hybrid pruning combines strategies across different components of LMMs. **SparseVLM** uses a rank-based strategy to set sparsification ratios adaptively and recycles pruned tokens into compact representations (Zhang et al., 2025b). **MustDrop** evaluates token importance across visual encoding, prefill, and decode, applying stage-specific strategies to remove redundancy and reduce computation (Liu et al., 2024a).

### 3.2 DATASETS

To systematically assess the impact of pruning techniques on LMMs, we conduct experiments on ten benchmark datasets covering six capability dimensions: (1) **Comprehensive Evaluation**: MME (Fu et al., 2023), and MMBench (Liu et al., 2024b); (2) **Mathematical Reasoning**: MathVista (Lu et al., 2024), and Math-Vision (Wang et al., 2025); (3) **Optical Character Recognition**: SEED-Bench-2-Plus (Li et al., 2024), and OCRBench (Liu et al., 2023b); (4) **Instruction Following**: MIA-Bench (Qian et al., 2024); (5) **Multidisciplinary Knowledge**: ScienceQA (Lu et al., 2022); (6) **Hallucination**: POPE (Li et al., 2023), and HallusionBench (Guan et al., 2024). Our dataset selection follows the capability dimensions identified in MME-Survey (Fu et al., 2024), ensuring coverage of core competencies such as visual–language understanding, cross-modal reasoning, and instruction following, skills central to current LMM research and applications.

### 3.3 BASE MODEL

Following prior work (Zhang et al., 2025b; Liu et al., 2024a; Bi et al., 2025a), we evaluate five representative open-source LMMs from three model families, namely LLaVA-v1.5-7B, InternVL3-1B, InternVL3-8B, Qwen2.5-VL-3B and Qwen2.5-VL-7B. These models align vision and language by integrating advanced visual and textual components. Typically, a visual encoder (e.g., CLIP) processes image inputs, while a large language model (e.g., Qwen) handles textual inputs. The extracted features are then fused via Multilayer Perceptron (MLP) connectors, enabling effective multimodal reasoning and alignment. Previous studies typically conduct experiments on only one or two model families, whereas we evaluate models across all three families.

### 3.4 EVALUATION METRICS

We consider multiple metrics in this benchmark. **Accuracy** serves as a basic evaluation metric, complemented by **performance drop** measured before and after token compression. To reflect practical considerations, we also record **total running time**, the time required for the entire process,

Table 1: Performance comparison across different methods and benchmarks on LLaVA-v1.5-7B.

Methods	Comprehensive			OCR		Multidisciplinary	Hallucination	Avg.
	MME	MMB-cn	MMB-en	SEED	OCR-B	Science QA	POPE	
<b>LLaVA-v1.5-7B</b>								
Vanilla	48.1	43.5	63.6	38.8	30.2	68.2	80.1	53.2
<i>Upper Bound: 576 Tokens (100%)</i>								
<b>Random</b>	<b>44.3 ± 1.8</b>	<b>39.4 ± 2.1</b>	<b>57.1 ± 2.6</b>	<b>38.3 ± 2.2</b>	<b>21.6 ± 2.1</b>	<b>65.7 ± 1.3</b>	<b>82.1 ± 0.3</b>	52.3
VTW	23.3	0.8	21.0	36.9	0.9	63.1	4.9	21.6
PruMerge	44.0	6.0	57.1	38.3	23.4	66.5	74.5	44.3
FastV	44.9	23.1	60.5	37.2	27.0	68.1	74.8	47.9
DivPrune	<b>49.2</b>	12.3	60.4	38.5	28.4	67.6	<b>86.4</b>	49.0
VisPrune	47.3	18.8	61.6	38.3	<b>29.1</b>	68.0	85.2	49.8
DART	46.8	25.8	61.7	37.8	28.3	66.3	83.2	50.0
MustDrop	47.8	41.3	61.0	37.9	28.9	67.6	80.1	52.1
SparseVLM	47.7	<b>44.0</b>	<b>61.7</b>	39.7	28.1	67.4	80.6	<b>52.7</b>
<i>Retain Averaged 192 Tokens (↓ 66.7%)</i>								
<b>Random</b>	<b>45.2 ± 0.3</b>	<b>37.1 ± 0.9</b>	<b>54.2 ± 1.2</b>	<b>38.1 ± 1.0</b>	<b>20.2 ± 2.8</b>	<b>64.0 ± 0.3</b>	<b>81.6 ± 0.3</b>	50.4
VTW	24.7	1.1	23.5	36.9	1.0	64.5	0.0	21.7
PruMerge	41.5	4.8	55.4	38.6	23.7	67.6	69.8	43.1
FastV	41.9	20.7	57.8	36.9	25.4	<b>68.3</b>	67.5	45.5
DivPrune	<b>48.9</b>	9.0	59.5	39.1	27.9	67.5	<b>86.4</b>	48.3
VisPrune	47.9	14.5	60.3	38.3	29.4	67.8	83.9	48.9
DART	46.1	22.4	61.0	37.6	26.7	67.1	79.9	48.7
MustDrop	47.4	41.7	61.1	39.6	<b>29.6</b>	67.5	78.9	52.3
SparseVLM	<b>48.9</b>	<b>48.2</b>	<b>62.4</b>	<b>39.9</b>	24.9	67.4	83.1	<b>53.5</b>
<i>Retain Averaged 128 Tokens (↓ 77.8%)</i>								
<b>Random</b>	<b>45.2 ± 0.3</b>	<b>37.1 ± 0.9</b>	<b>54.2 ± 1.2</b>	<b>38.1 ± 1.0</b>	<b>20.2 ± 2.8</b>	<b>64.0 ± 0.3</b>	<b>81.6 ± 0.3</b>	50.4
VTW	24.7	1.1	23.5	36.9	1.0	64.5	0.0	21.7
PruMerge	41.5	4.8	55.4	38.6	23.7	67.6	69.8	43.1
FastV	41.9	20.7	57.8	36.9	25.4	<b>68.3</b>	67.5	45.5
DivPrune	<b>48.9</b>	9.0	59.5	39.1	27.9	67.5	<b>86.4</b>	48.3
VisPrune	47.9	14.5	60.3	38.3	29.4	67.8	83.9	48.9
DART	46.1	22.4	61.0	37.6	26.7	67.1	79.9	48.7
MustDrop	47.4	41.7	61.1	39.6	<b>29.6</b>	67.5	78.9	52.3
SparseVLM	<b>48.9</b>	<b>48.2</b>	<b>62.4</b>	<b>39.9</b>	24.9	67.4	83.1	<b>53.5</b>
<i>Retain Averaged 64 Tokens (↓ 88.9%)</i>								
<b>Random</b>	<b>42.2 ± 0.2</b>	<b>7.3 ± 3.6</b>	<b>52.4 ± 1.1</b>	<b>36.5 ± 2.7</b>	<b>18.4 ± 2.5</b>	<b>62.2 ± 0.9</b>	<b>74.9 ± 0.2</b>	42.6
VTW	25.0	4.4	50.0	38.3	1.4	65.7	9.2	27.7
PruMerge	41.2	4.5	53.1	38.8	22.8	67.8	65.1	41.9
FastV	32.2	12.7	45.8	36.2	16.8	67.2	51.3	37.5
DivPrune	<b>48.1</b>	6.1	57.9	<b>39.0</b>	26.9	65.9	<b>85.3</b>	<b>47.0</b>
VisPrune	47.8	7.5	58.2	38.6	<b>28.1</b>	67.5	80.7	46.9
DART	42.8	<b>17.4</b>	57.4	37.6	23.4	67.9	71.0	45.4
MustDrop	43.9	13.2	57.4	38.0	24.8	<b>68.5</b>	67.2	44.7
SparseVLM	45.5	15.7	<b>58.8</b>	38.1	16.7	67.8	76.8	45.6

and **compression strategy time**, the time spent solely on token pruning, and **prefilling-phase time**, the forward pass that processes image and text tokens before the first decoding step.

## 4 EXPERIMENTS

### 4.1 IMPLEMENTATION DETAILS

We implemented UniPruneBench in PyTorch and conducted all experiments on NVIDIA A100 GPUs. For benchmark execution across baselines and models, we employed the open-source toolkit VLMEvalKit (Duan et al., 2024a). Unless otherwise specified, all results are reported with a batch

Table 2: Performance comparison across different methods and benchmarks on InternVL3-8B.

Methods	Comprehensive		OCR	Multidisciplinary	Hallucination		Mathematical		Instruction	Avg.
	MME	MMB-en	SEED	Science QA	POPE	Hallus	Math-V	MathVista	MIA	
<b>InternVL3-8B</b>										
Vanilla	86.44	85.80	69.52	98.07	90.33	49.80	69.70	28.29	72.22	70.02
<i>Upper Bound, 100% Tokens (100%)</i>										
<i>Retain Averaged 33.3% Tokens (↓ 66.7%)</i>										
<b>Random-Pre</b>	77.21	78.79	56.65	90.00	88.58	37.25	50.00	22.70	80.93	64.68
	↓10.7%	↓8.2%	↓18.5%	↓8.2%	↓1.9%	↓25.2%	↓28.3%	↓19.8%	↑12.1%	
<b>Random-Intra</b>	81.04	82.00	60.00	94.00	89.70	41.09	53.90	27.63	74.50	67.10
	↓6.2%	↓4.4%	↓13.7%	↓4.2%	↓0.7%	↓17.5%	↓22.7%	↓2.3%	↑3.2%	
<b>FastV</b>	80.60	83.00	58.00	92.00	90.21	42.95	49.80	24.34	74.74	66.18
	↓6.8%	↓3.3%	↓16.6%	↓6.2%	↓0.1%	↓13.8%	↓28.6%	↓14.0%	↑3.5%	
<b>DivPrune</b>	81.76	<b>84.00</b>	<b>63.00</b>	95.00	90.09	44.08	60.50	<b>26.97</b>	79.66	69.45
	↓5.4%	↓2.1%	↓9.4%	↓3.1%	↓0.3%	↓11.5%	↓13.2%	↓4.7%	↑10.3%	
<b>GPrune</b>	<b>82.62</b>	83.00	62.00	<b>96.00</b>	<b>90.12</b>	<b>46.91</b>	<b>64.60</b>	26.97	<b>81.61</b>	<b>70.43</b>
	↓4.4%	↓3.3%	↓10.8%	↓2.1%	↓0.2%	↓5.8%	↓7.3%	↓4.7%	↑13.0%	
<i>Retain Averaged 22.2% Tokens (↓ 77.8%)</i>										
<b>Random-Pre</b>	77.30	77.00	55.00	88.00	88.08	35.52	47.60	21.38	77.34	62.91
	↓10.6%	↓10.2%	↓20.9%	↓10.2%	↓2.5%	↓28.7%	↓31.7%	↓24.4%	↑7.1%	
<b>Random-Intra</b>	78.13	79.00	57.00	91.00	88.93	38.24	48.10	22.04	72.69	63.90
	↓9.6%	↓7.9%	↓18.0%	↓7.1%	↓1.6%	↓23.2%	↓31.0%	↓22.1%	↑0.6%	
<b>FastV</b>	79.40	83.00	56.00	91.00	89.37	38.29	49.70	<b>26.32</b>	72.20	65.03
	↓8.1%	↓3.3%	↓19.4%	↓7.1%	↓1.1%	↓23.1%	↓28.7%	↓7.0%	↓0.01%	
<b>GPrune</b>	78.97	79.00	<b>60.00</b>	<b>94.00</b>	89.33	43.70	55.50	24.01	74.70	66.58
	↓8.6%	↓7.9%	↓13.7%	↓4.1%	↓1.1%	↓12.3%	↓20.4%	↓15.1%	↑3.4%	
<b>DivPrune</b>	<b>80.25</b>	<b>83.00</b>	<b>60.00</b>	93.00	<b>90.18</b>	<b>42.64</b>	<b>56.00</b>	23.36	<b>79.82</b>	<b>67.58</b>
	↓7.2%	↓3.3%	↓13.7%	↓5.1%	↓0.2%	↓14.4%	↓19.7%	↓17.4%	↑10.5%	
<i>Retain Averaged 11.1% Tokens (↓ 88.9%)</i>										
<b>Random-Pre</b>	73.11	72.00	52.00	85.00	86.32	34.72	44.00	21.38	77.93	60.72
	↓15.4%	↓16.1%	↓25.2%	↓13.3%	↓4.4%	↓30.3%	↓36.9%	↓24.4%	↑7.8%	
<b>Random-Intra</b>	72.97	72.00	52.00	86.00	86.61	34.47	44.90	24.67	71.97	60.73
	↓15.6%	↓16.1%	↓25.2%	↓12.2%	↓4.1%	↓30.8%	↓35.6%	↓12.8%	↓0.3%	
<b>FastV</b>	<b>76.49</b>	80.00	54.00	89.00	88.00	34.88	47.00	22.04	68.97	62.26
	↓11.5%	↓6.8%	↓22.3%	↓9.2%	↓2.6%	↓30.0%	↓32.6%	↓22.1%	↓4.5%	
<b>GPrune</b>	70.82	71.00	55.00	88.00	85.35	36.68	47.90	<b>26.32</b>	<b>88.71</b>	63.31
	↓18.1%	↓17.3%	↓20.9%	↓10.2%	↓5.5%	↓26.3%	↓31.2%	↓7.0%	↑22.8%	
<b>DivPrune</b>	75.79	<b>81.00</b>	<b>56.00</b>	<b>90.00</b>	<b>88.95</b>	<b>38.13</b>	<b>49.20</b>	<b>26.32</b>	70.97	<b>64.04</b>
	↓12.3%	↓5.6%	↓19.4%	↓8.2%	↓1.5%	↓23.4%	↓29.4%	↓7.0%	↓1.8%	

size of 1. We evaluate performance under different pruning ratios, ensuring that pruned models maintain sufficiently high accuracy for meaningful comparison with baselines. To enable fair comparisons across benchmarks of varying scales, we report both average accuracy and relative performance. To ensure a fair comparison across all Intra-LLM pruning strategies, we fix the pruning location inside the large model at layer  $K = 2$  for every method. For clarity, Random-Pre denotes uniform random dropping applied to visual tokens before they enter the LLM (Pre-LLM stage), whereas Random-Intra performs the same stochastic removal inside the LLM (Intra-LLM stage); both retain exactly the target sparsity yet introduce no learned importance bias. For task performance metrics, we have normalized to 0-100 for MME to align with other datasets, with higher values indicating better results, while for runtime measurements, lower values are preferable. To simplify presentation, we adopt the following dataset abbreviations when reporting results: MMBench as MMB, Math-Vision as Math-V, SEEDBench-2-Plus as SEED, OCRBench as OCR-B, MIA-Bench as MIA, and HallusionBench as Hallus.

## 4.2 MAIN RESULTS

The comparison results of different methods are shown in Table 1, Table 2, and Table 3. Based on these results, several key findings emerge:

**1. Random pruning remains a surprisingly strong baseline.** Random pruning consistently outperforms several well-designed methods, such as GPrune, VTw, and PruMerge. For instance, On LLaVA-v1.5-7B, six out of eight perform worse than random pruning at 66.7% and 77.8% pruning

Table 3: Performance comparison across different methods and benchmarks on Qwen2.5-VL-7B.

Methods	Comprehensive		OCR		Multidisciplinary		Hallucination		Mathematical		Instruction	Avg.
	MME	MMB-en	SEED	OCR-B	Science QA	POPE	Hallus	Math-V	MathVista	MIA		
<b>Qwen2.5-VL-7B</b>												<i>Upper Bound: 100% Token (100%)</i>
Vanilla	82.5	79.8	69.6	78.3	89.0	87.5	47.5	24.3	63.9	70.2	69.3	
<i>Retain Averaged 33.3% Tokens (↓ 66.7%)</i>												
FastV	69.4	74.1	59.0	50.5	<b>80.0</b>	83.7	37.9	9.34	40.2	60.9	56.5	
Random-Intra	67.7	74.7	58.0	53.3	79.0	81.9	38.6	9.51	41.0	61.9	56.6	
GPrune	68.6	71.2	57.0	54.9	<b>80.0</b>	<b>84.4</b>	37.8	<b>9.8</b>	47.8	60.10	57.2	
Random-Pre	71.9	71.2	57.0	54.9	<b>80.0</b>	<b>84.4</b>	37.8	9.41	45.7	<b>62.9</b>	57.5	
DART	71.8	<b>76.5</b>	54.0	58.2	<b>80.0</b>	81.9	<b>41.6</b>	9.1	43.3	61.69	57.8	
DivPrune	<b>72.3</b>	73.7	<b>63.0</b>	<b>65.4</b>	79.0	84.3	<b>41.6</b>	9.57	<b>48.3</b>	61.5	<b>59.8</b>	
<i>Retain Averaged 22.2% Tokens (↓ 77.8%)</i>												
GPrune	59.8	65.1	52.0	38.1	78.0	80.6	31.5	<b>9.8</b>	47.5	60.71	52.3	
FastV	66.4	70.6	55.0	36.4	78.0	80.7	35.6	9.21	38.1	60.3	53.0	
Random-Intra	64.7	71.0	53.0	45.6	78.0	80.1	36.2	8.55	38.0	62.3	53.7	
Random-Pre	67.9	69.3	54.0	45.6	78.0	79.9	34.2	9.67	45.5	<b>63.0</b>	54.7	
DART	68.4	<b>74.5</b>	50.0	50.7	<b>80.0</b>	79.9	<b>40.0</b>	9.6	40.1	60.83	55.4	
DivPrune	<b>70.0</b>	73.0	<b>59.0</b>	<b>57.5</b>	79.0	<b>82.8</b>	37.1	9.8	<b>47.7</b>	61.3	<b>57.7</b>	
<i>Retain Averaged 11.1% Tokens (↓ 88.9%)</i>												
FastV	51.4	53.2	47.0	18.9	74.0	69.2	29.3	8.98	30.3	58.2	44.0	
GPrune	49.9	53.7	46.0	16.4	71.0	70.0	24.4	9.24	47.4	60.3	44.8	
Random-Intra	62.5	68.3	47.0	31.1	75.0	74.5	32.4	8.09	31.9	61.3	49.2	
Random-Pre	64.1	64.8	48.0	31.7	73.0	73.4	27.7	9.80	45.3	<b>62.7</b>	50.1	
DART	62.2	<b>70.7</b>	46.0	37.7	<b>79.0</b>	73.2	<b>34.8</b>	<b>9.90</b>	33.9	62.6	51.0	
DivPrune	<b>64.6</b>	68.6	<b>51.0</b>	<b>40.8</b>	76.0	<b>78.3</b>	30.8	8.95	<b>47.9</b>	62.22	<b>52.9</b>	

ratios. This unexpected result highlights the limitation of current designs and suggests that more effective pruning strategies are needed beyond naive baselines.

**2. No single method achieves universal superiority.** No approach dominates across all models and pruning ratios. DivPrune achieves the best results on both Qwen2.5-VL-7B and InternVL3-8B under all ratios. However, on LLaVA-v1.5-7B, SparseVLM surpasses DivPrune under light pruning ratios, while DivPrune regains superiority under more aggressive pruning. This indicates that performance strongly depends on both the model architecture and the pruning level.

**3. Hybrid-based methods demonstrate strong overall performance.** Among the three categories of methods, hybrid-based approaches achieve the best results on LLaVA-v1.5-7B at the 77.8% and 66.7% pruning ratios, though they perform worse at the 88.9% ratio. On InternVL3-8B and Qwen2.5-VL-7B, ViT-only methods (e.g., DivPrune) consistently outperform LLM-only methods, suggesting that vision-side pruning is more effective than language-side pruning.

**4. Task-level sensitivity varies: instruction following improves, while OCR degrades severely.** Most benchmarks show accuracy degradation as pruning intensifies. However, instruction-following tasks (e.g., MIA) exhibit improvements in some cases. For example, on InternVL3-8B, DivPrune raises accuracy from 72.22% to 79.82%. We hypothesize that pruning increases the relative weight of textual inputs, thereby enhancing instruction adherence. In contrast, OCR tasks are highly sensitive to pruning: as more visual tokens are removed, crucial details are lost, leading to rapid performance decline.

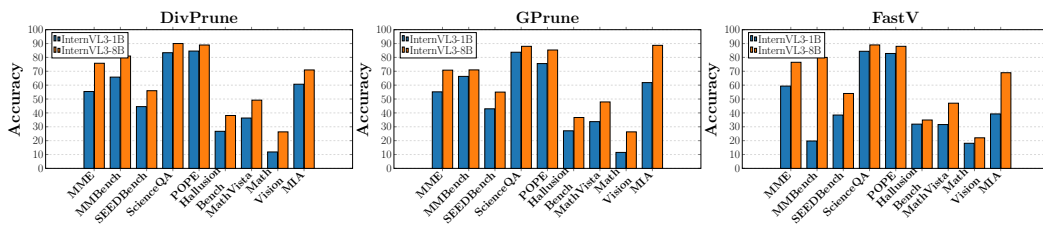


Figure 3: Performance Comparison of different model sizes for InternVL3 at 88.9% pruning rate.

**5. Higher pruning ratios induce sharper performance loss.** Light pruning leads to moderate degradation, while aggressive pruning causes substantial drops. For example, on Qwen2.5-VL-7B, the average accuracy decreases from 57.5% at 33% tokens to 50.1% at 11% tokens under random pruning. Similarly, on InternVL3-8B, DivPrune maintains 67.58% at 22% tokens but falls to 64.04% at 11% tokens. Notably, DivPrune consistently achieves the best results under the highest pruning ratio (88.9%), showing stronger robustness in extreme scenarios.

**6. Consistent cross-model trends.** Despite architectural differences, all three models exhibit similar behaviors: random pruning is unexpectedly competitive, OCR tasks are highly fragile, instruction-following tasks remain robust, and no single method dominates universally.

### 4.3 ANALYSIS AND DISCUSSION

**Influence of model size** To investigate the sensitivity of token compression techniques to model scale, we evaluate three representative methods, DivPrune, GPrune, and FastV, across two variants of InternVL: InternVL3-1B (small) and InternVL3-8B (large). As shown in Fig 3, scaling up the base model consistently yields significant accuracy gains across nearly all benchmarks under all compression methods, confirming that larger models retain more semantic capacity even after token reduction. The results indicate that larger architectures provide greater robustness to token reduction, suggesting that compression strategies should be evaluated across scales rather than in isolation.

**Running time** Considering real-world scenarios, we also evaluate the running time of different pruning methods. We profile three nested intervals: **Total time**, the elapsed time to finish the entire dataset; **Prefill time**, the single encoder forward pass that computes keys and values for all visual and textual tokens before any decoding starts, a phase that is compute-bound for the large model; and **Method time**, the GPU milliseconds spent only on the compression subroutine (token scoring, selection and tensor re-layout). All measurements were collected on an NVIDIA A100-40 GB GPU with batch size = 1 and three independent runs. All reported methods correspond to a uniform pruning rate of 88.9% on the MME benchmark. The results in Table 4 show that the last component never exceeds 0.5s, less than 0.12 % of the corresponding total. So the cost of importance estimation is negligible. Pruning therefore exerts its effect entirely within the prefill: DivPrune and GPrune shorten it from 320 s to 185 s and 167 s, delivering 1.73–1.92× encoder acceleration and an overall 1.62–1.68× end-to-end speed-up versus the vanilla model.

Table 4: The running time comparison of different methods on InternVL3-8B

Methods	Total time (sec)	Prefill time (sec)	Method time (sec)
Vallania	761.00	320.00	<b>0.00</b>
Random-pre	491.00	201.00	<b>0.11</b>
Random-intra	481.00	209.00	0.12
Fastv	497.00	212.00	0.33
DivPrune	469.00	185.00	0.32
GPrune	<b>454.00</b>	<b>167.00</b>	0.47

**Combination of different pruning strategies** To examine whether the same overall sparsity should be applied in one step or decomposed, we fix the global pruning ratio at 88.9% and realize it through two design choices: **Single-stage**, a single 88.9% drop executed either before the LLM (Pre-LLM) or inside the LLM (Intra-LLM). **Two-stage**, a 66.7% Pre-LLM pruning followed by 66.7% Intra-LLM pruning, giving the same compound retention. Contrary to the “more-is-better” intuition, Table 5

432 **Table 5: Performance comparison for the combination of different pruning strategies on**  
 433 **InternVL3-8B.** All methods achieve 88.9% pruning rate. Mixed methods use two-stage pruning.

435 Pre-LLM	436 Intra-LLM	Comprehensive		OCR	Multidisciplinary		Hallucination		Mathematical		Instruction	437 Avg.	
		MME	MMB	SEED	Science QA	POPE	Hallus	Math-V	MathVista	MIA			
<b>438 InternVL3-8B</b>													
Vanilla		86.44	85.80	69.52		98.07	90.33	49.80	69.70	28.29	72.22	70.02	
<i>439 Retain Averaged 11.1% Tokens (↓ 88.9%)</i>													
440 <b>X</b>	441 <b>Random</b>	72.97	72.00	52.00		86.00	86.61	34.47	44.90	24.67	71.97	60.62	
		↓15.6%	↓16.1%	↓25.2%		↓12.2%	↓4.1%	↓30.8%	↓35.6%	↓12.8%	↓0.3%		
442 <b>Random</b>	443 <b>X</b>	73.11	72.00	52.00		85.00	86.32	34.72	44.00	21.38	77.93	60.72	
		↓15.4%	↓16.1%	↓25.2%		↓13.3%	↓4.4%	↓30.3%	↓36.9%	↓24.4%	↑7.8%		
444 <b>X</b>	445 <b>FastV</b>	76.49	80.00	54.00		89.00	88.00	34.88	47.00	22.04	68.97	62.26	
		↓11.5%	↓6.8%	↓22.3%		↓9.2%	↓2.6%	↓30.0%	↓32.6%	↓22.1%	↓4.5%		
446 <b>GPrune</b>	447 <b>X</b>	70.82	71.00	55.00		88.00	85.35	36.68	47.90	26.32	88.71	63.31	
		↓18.1%	↓17.3%	↓20.9%		↓10.2%	↓5.5%	↓26.3%	↓31.2%	↓7.0%	↑22.8%		
448 <b>DivPrune</b>	449 <b>X</b>	75.79	<b>81.00</b>	<b>56.00</b>		<b>90.00</b>	<b>88.95</b>	<b>38.13</b>	49.20	<b>26.32</b>	70.97	<b>64.04</b>	
		↓12.3%	↓5.6%	↓19.4%		↓8.2%	↓1.5%	↓23.4%	↓29.4%	↓7.0%	↓1.8%		
450 <b>Random</b>	451 <b>Random</b>	73.72	72.0	51.9		84.6	86.4	34.5	45.6	10.29	69.8	58.76	
		↓35.4%	↓16.1%	↓25.4%		↓13.7%	↓4.3%	↓30.7%	↓34.6%	↓63.6%	↓3.4%		
452 <b>DivPrune</b>	453 <b>Random</b>	74.24	73.5	53.0		87.3	87.5	37.1	47.4	10.68	71.0	60.19	
		↓33.0%	↓14.3%	↓23.7%		↓11.0%	↓3.1%	↓25.5%	↓32.0%	↓62.2%	↓1.7%		
454 <b>GPrune</b>	455 <b>Random</b>	77.57	74.6	53.4		89.4	87.6	37.2	50.3	10.03	68.7	60.98	
		↓32.0%	↓13.1%	↓23.1%		↓8.8%	↓3.0%	↓25.3%	↓27.8%	↓64.5%	↓4.9%		
456 <b>Random</b>	457 <b>FastV</b>	77.89	77.7	54.1		88.0	87.7	36.1	48.8	10.49	70.3	61.23	
		↓30.8%	↓9.4%	↓22.2%		↓10.2%	↓2.9%	↓27.5%	↓30.0%	↓62.9%	↓2.6%		
458 <b>GPrune</b>	459 <b>FastV</b>	76.97	77.4	53.9		88.2	87.6	37.4	48.0	9.96	71.7	61.24	
		↓31.6%	↓9.8%	↓22.5%		↓10.0%	↓3.0%	↓24.9%	↓31.1%	↓64.8%	↓0.7%		
460 <b>DivPrune</b>	461 <b>FastV</b>	<b>77.97</b>	80.1	54.2		89.7	88.5	37.4	<b>50.3</b>	10.66	72.6	62.38	
		↓31.5%	↓6.6%	↓22.0%		↓8.5%	↓2.0%	↓28.3%	↓30.3%	↓62.3%	↓1.8%		

457 reveals that simply chaining two existing pruning stages underperforms the stronger single-stage  
 458 baseline: the best solitary Pre-LLM method (64.04%) still surpasses every 66.7% × 66.7% hybrid  
 459 method, despite the latter retaining the same number of tokens. This outcome indicates that naïvely  
 460 concatenating off-the-shelf pruning criteria does not guarantee additive gains. Instead, an effective  
 461 combination requires a deliberate design that respects the complementary nature of each stage as  
 462 well as the downstream scenario. Without such targeted orchestration, it may be that the second  
 463 stage often re-discards already informative tokens, leading to sub-optimal performance even though  
 464 the aggregate sparsity is unchanged.

## 465 5 CONCLUSION

466 In this paper, we introduced UniPruneBench, a unified benchmark for evaluating visual token pruning  
 467 methods in large multimodal models. By systematically covering diverse datasets, model families,  
 468 pruning algorithms, and system-level efficiency metrics, UniPruneBench addresses the limitations  
 469 of prior fragmented and non-standardized evaluations. Our results reveal surprising trends,  
 470 including the competitiveness of random pruning, the lack of a universally superior method, and the  
 471 task-specific vulnerabilities of pruning strategies. These insights highlight both the challenges and  
 472 opportunities for designing more effective token compression methods. We hope UniPruneBench  
 473 not only facilitates fair comparison and reproducibility but also inspires future advances in efficient  
 474 multimodal learning and deployment.

## 475 ETHICS STATEMENT

476 Our **UniPruneBench** benchmark is designed to provide a standardized, fair, and reproducible evaluation  
 477 of visual token pruning methods in large multimodal models. The benchmark itself does not  
 478 generate content or make decisions, and thus poses minimal direct ethical risk. However, potential  
 479 considerations include:

480 **1. Data sources and bias:** UniPruneBench relies on existing public datasets, which may contain  
 481 inherent biases in terms of demographics, languages, or visual concepts. Users should be aware that  
 482 these biases may affect model evaluation outcomes.

486 2. **Misuse of results:** While the benchmark aims to improve efficiency in multimodal models,  
 487 it could indirectly enable faster deployment of models in sensitive applications. We encourage  
 488 responsible use and adherence to ethical AI guidelines.

489 3. **User queries and prompts:** Models evaluated on UniPruneBench could still produce harmful or  
 490 inappropriate outputs in response to malicious or unsafe queries. The benchmark does not mitigate  
 491 such risks, and appropriate safeguards should be implemented by users.

492 Overall, UniPruneBench aims to advance research in efficient multimodal modeling in a safe and  
 493 responsible manner, providing transparency and reproducibility while minimizing ethical concerns.

## 496 REPRODUCIBILITY STATEMENT

497 We provide full details to ensure that all experiments in this paper are reproducible. The code of  
 498 UniPruneBench is shown in the appendix, including standardized evaluation scripts and token prun-  
 499 ing implementations. All datasets used are publicly available, and we specify dataset preprocessing,  
 500 prompt templates, token retention ratios, and system-level measurement protocols. Additionally, we  
 501 include instructions for reproducing results across different model families (LLaVA, Intern-VL, and  
 502 Qwen-VL) and pruning methods. By releasing the benchmark and evaluation pipeline, we aim to  
 503 enable fair comparison, facilitate further research, and ensure transparency in reported findings.

## 506 REFERENCES

507 Saeed Ranjbar Alvar, Gursimran Singh, Mohammad Akbari, and Yong Zhang. Divprune: Diversity-  
 508 based visual token pruning for large multimodal models. In *Proceedings of the Computer Vision*  
 509 and *Pattern Recognition Conference*, pp. 9392–9401, 2025.

511 Shuai Bai, Keqin Chen, Xuejing Liu, Jialin Wang, Wenbin Ge, Sibo Song, Kai Dang, Peng Wang,  
 512 Shijie Wang, Jun Tang, et al. Qwen2.5-vl technical report. *arXiv preprint arXiv:2502.13923*,  
 513 2025.

514 Jinhe Bi, Yifan Wang, Danqi Yan, Xun Xiao, Artur Hecker, Volker Tresp, and Yunpu Ma. Prism:  
 515 Self-pruning intrinsic selection method for training-free multimodal data selection. *arXiv preprint*  
 516 *arXiv:2502.12119*, 2025a.

518 Jinhe Bi, Yujun Wang, Haokun Chen, Xun Xiao, Artur Hecker, Volker Tresp, and Yunpu Ma.  
 519 LLaVA steering: Visual instruction tuning with 500x fewer parameters through modality linear  
 520 representation-steering. In Wanxiang Che, Joyce Nabende, Ekaterina Shutova, and Mo-  
 521 hammad Taher Pilehvar (eds.), *Proceedings of the 63rd Annual Meeting of the Association for*  
 522 *Computational Linguistics (Volume 1: Long Papers)*, pp. 15230–15250, Vienna, Austria, July  
 523 2025b. Association for Computational Linguistics. ISBN 979-8-89176-251-0. URL <https://aclanthology.org/2025.acl-long.739/>.

525 Jinhe Bi, Danqi Yan, Yifan Wang, Wenke Huang, Haokun Chen, Guancheng Wan, Mang Ye, Xun  
 526 Xiao, Hinrich Schuetze, Volker Tresp, et al. Cot-kinetics: A theoretical modeling assessing lrm  
 527 reasoning process. *arXiv preprint arXiv:2505.13408*, 2025c.

528 Daniel Bolya, Cheng-Yang Fu, Xiaoliang Dai, Peizhao Zhang, Christoph Feichtenhofer, and Judy  
 529 Hoffman. Token merging: Your vit but faster. In *ICLR*, 2023.

531 Davide Caffagni, Federico Cocchi, Luca Barsellotti, Nicholas Moratelli, Sara Sarto, Lorenzo  
 532 Baraldi, Marcella Cornia, and Rita Cucchiara. The revolution of multimodal large language mod-  
 533 els: a survey. *ACL*, 2024.

534 Liang Chen, Haozhe Zhao, Tianyu Liu, Shuai Bai, Junyang Lin, Chang Zhou, and Baobao Chang.  
 535 An image is worth 1/2 tokens after layer 2: Plug-and-play inference acceleration for large vision-  
 536 language models. In *European Conference on Computer Vision*, pp. 19–35. Springer, 2024a.

538 Yi Chen, Jian Xu, Xu-Yao Zhang, Wen-Zhuo Liu, Yang-Yang Liu, and Cheng-Lin Liu. Recoverable  
 539 compression: A multimodal vision token recovery mechanism guided by text information. In  
*Proceedings of the AAAI Conference on Artificial Intelligence*, volume 39, pp. 2293–2301, 2025.

540 Zhe Chen, Weiyun Wang, Yue Cao, Yangzhou Liu, Zhangwei Gao, Erfei Cui, Jinguo Zhu, Shen-  
 541 glong Ye, Hao Tian, Zhaoyang Liu, et al. Expanding performance boundaries of open-source  
 542 multimodal models with model, data, and test-time scaling. *arXiv preprint arXiv:2412.05271*,  
 543 2024b.

544 Alexey Dosovitskiy, Lucas Beyer, Alexander Kolesnikov, Dirk Weissenborn, Xiaohua Zhai, Thomas  
 545 Unterthiner, Mostafa Dehghani, Matthias Minderer, Georg Heigold, Sylvain Gelly, et al. An  
 546 image is worth 16x16 words: Transformers for image recognition at scale. *ICLR*, 2020.

547

548 Haodong Duan, Junming Yang, Yuxuan Qiao, Xinyu Fang, Lin Chen, Yuan Liu, Xiaoyi Dong,  
 549 Yuhang Zang, Pan Zhang, Jiaqi Wang, et al. Vlmevalkit: An open-source toolkit for evaluat-  
 550 ing large multi-modality models. In *Proceedings of the 32nd ACM international conference on*  
 551 *multimedia*, pp. 11198–11201, 2024a.

552 Haodong Duan, Junming Yang, Yuxuan Qiao, Xinyu Fang, Lin Chen, Yuan Liu, Xiaoyi Dong,  
 553 Yuhang Zang, Pan Zhang, Jiaqi Wang, et al. Vlmevalkit: An open-source toolkit for evaluat-  
 554 ing large multi-modality models. In *Proceedings of the 32nd ACM international conference on*  
 555 *multimedia*, pp. 11198–11201, 2024b.

556 Yuxiang Duan, Ao Li, Yingqin Li, Luyu Li, and Pengwei Wang. Gridprune: From “where to look”  
 557 to “what to select” in visual token pruning for mllms. *arXiv preprint arXiv:2511.10081*, 2025.

558

559 Yue Fan, Xiaojian Ma, Rujie Wu, Yuntao Du, Jiaqi Li, Zhi Gao, and Qing Li. Videoagent: A  
 560 memory-augmented multimodal agent for video understanding. In *European Conference on Com-  
 561 puter Vision*, pp. 75–92. Springer, 2024.

562 Chaoyou Fu, Peixian Chen, Yunhang Shen, Yulei Qin, Mengdan Zhang, Xu Lin, Jinrui Yang, Xiawu  
 563 Zheng, Ke Li, Xing Sun, et al. Mme: A comprehensive evaluation benchmark for multimodal  
 564 large language models. *arXiv:2306.13394*, 2023.

565

566 Chaoyou Fu, Yi-Fan Zhang, Shukang Yin, Bo Li, Xinyu Fang, Sirui Zhao, Haodong Duan, Xing  
 567 Sun, Ziwei Liu, Liang Wang, et al. Mme-survey: A comprehensive survey on evaluation of  
 568 multimodal llms. *arXiv preprint arXiv:2411.15296*, 2024.

569

570 Zhi Gao, Yuntao Du, Xintong Zhang, Xiaojian Ma, Wenjuan Han, Song-Chun Zhu, and Qing Li.  
 571 Clova: A closed-loop visual assistant with tool usage and update. In *Proceedings of the IEEE/CVF*  
 572 *Conference on Computer Vision and Pattern Recognition*, pp. 13258–13268, 2024.

573

574 Aaron Grattafiori, Abhimanyu Dubey, Abhinav Jauhri, Abhinav Pandey, Abhishek Kadian, Ahmad  
 575 Al-Dahle, Aiesha Letman, Akhil Mathur, Alan Schelten, Alex Vaughan, et al. The llama 3 herd  
 576 of models. *arXiv preprint arXiv:2407.21783*, 2024.

577

578 Tianrui Guan, Fuxiao Liu, Xiyang Wu, Ruiqi Xian, Zongxia Li, Xiaoyu Liu, Xijun Wang, Lichang  
 579 Chen, Furong Huang, Yaser Yacoob, et al. Hallusionbench: an advanced diagnostic suite for  
 580 entangled language hallucination and visual illusion in large vision-language models. In *Pro-  
 581 ceedings of the IEEE/CVF Conference on Computer Vision and Pattern Recognition*, pp. 14375–  
 582 14385, 2024.

583

584 Tanmay Gupta and Aniruddha Kembhavi. Visual programming: Compositional visual reasoning  
 585 without training. In *Proceedings of the IEEE/CVF Conference on Computer Vision and Pattern*  
 586 *Recognition*, pp. 14953–14962, 2023.

587

588 Jiaxing Huang and Jingyi Zhang. A survey on evaluation of multimodal large language models.  
 589 *arXiv preprint arXiv:2408.15769*, 2024.

590

591 Lei Jiang, Zixun Zhang, Yuting Zeng, Chunzhao Xie, Tongxuan Liu, Zhen Li, Lechao Cheng, and  
 592 Xiaohua Xu. Dcp: Dual-cue pruning for efficient large vision-language models. In *Proceedings of*  
 593 *the 2025 Conference on Empirical Methods in Natural Language Processing*, pp. 21202–21215,  
 2025a.

594

595 Yutao Jiang, Qiong Wu, Wenhao Lin, Wei Yu, and Yiyi Zhou. What kind of visual tokens do  
 596 we need? training-free visual token pruning for multi-modal large language models from the  
 597 perspective of graph. In *Proceedings of the AAAI Conference on Artificial Intelligence*, volume 39,  
 598 pp. 4075–4083, 2025b.

594 Jihyung Kil, Zheda Mai, Justin Lee, Arpita Chowdhury, Zihe Wang, Kerrie Cheng, Lemeng Wang,  
 595 Ye Liu, and Wei-Lun Harry Chao. Mllm-compbench: A comparative reasoning benchmark for  
 596 multimodal llms. *Advances in Neural Information Processing Systems*, 37:28798–28827, 2024.

597

598 Bo Li, Yuanhan Zhang, Dong Guo, Renrui Zhang, Feng Li, Hao Zhang, Kaichen Zhang, Peiyuan  
 599 Zhang, Yanwei Li, Ziwei Liu, et al. Llava-onevision: Easy visual task transfer. *Transactions on  
 600 Machine Learning Research*, 2025.

601

602 Bohao Li, Yuying Ge, Yi Chen, Yixiao Ge, Ruimao Zhang, and Ying Shan. Seed-bench-2-plus:  
 603 Benchmarking multimodal large language models with text-rich visual comprehension. *arXiv  
 604 preprint arXiv:2404.16790*, 2024.

605

606 Yifan Li, Yifan Du, Kun Zhou, Jinpeng Wang, Wayne Xin Zhao, and Ji-Rong Wen. Evaluating  
 607 object hallucination in large vision-language models. In *Proceedings of the 2023 Conference on  
 608 Empirical Methods in Natural Language Processing*, pp. 292–305, 2023.

609

610 Zhihang Lin, Mingbao Lin, Luxi Lin, and Rongrong Ji. Boosting multimodal large language models  
 611 with visual tokens withdrawal for rapid inference. In *Proceedings of the AAAI Conference on  
 Artificial Intelligence*, volume 39, pp. 5334–5342, 2025.

612

613 Haotian Liu, Chunyuan Li, Qingyang Wu, and Yong Jae Lee. Visual instruction tuning. *Advances  
 614 in neural information processing systems*, 36:34892–34916, 2023a.

615

616 Ting Liu, Liangtao Shi, Richang Hong, Yue Hu, Quanjun Yin, and Linfeng Zhang. Multi-stage  
 617 vision token dropping: Towards efficient multimodal large language model, 2024a. URL <https://arxiv.org/abs/2411.10803>.

618

619 Yuan Liu, Haodong Duan, Yuanhan Zhang, Bo Li, Songyang Zhang, Wangbo Zhao, Yike Yuan,  
 620 Jiaqi Wang, Conghui He, Ziwei Liu, et al. Mmbench: Is your multi-modal model an all-around  
 621 player? In *European Conference on Computer Vision*, pp. 216–233. Springer, 2024b.

622

623 Yuliang Liu, Zhang Li, Biao Yang, Chunyuan Li, Xucheng Yin, Cheng-lin Liu, Lianwen Jin,  
 624 and Xiang Bai. On the hidden mystery of ocr in large multimodal models. *arXiv preprint  
 625 arXiv:2305.07895*, 2023b.

626

627 Pan Lu, Swaroop Mishra, Tanglin Xia, Liang Qiu, Kai-Wei Chang, Song-Chun Zhu, Oyvind Tafjord,  
 628 Peter Clark, and Ashwin Kalyan. Learn to explain: Multimodal reasoning via thought chains for  
 629 science question answering. *Advances in Neural Information Processing Systems*, 35:2507–2521,  
 2022.

630

631 Pan Lu, Hritik Bansal, Tony Xia, Jiacheng Liu, Chunyuan Li, Hannaneh Hajishirzi, Hao Cheng, Kai-  
 632 Wei Chang, Michel Galley, and Jianfeng Gao. Mathvista: Evaluating mathematical reasoning  
 633 of foundation models in visual contexts. In *The Twelfth International Conference on Learning  
 634 Representations*, 2024.

635

636 Yusu Qian, Hanrong Ye, Jean-Philippe Fauconnier, Peter Grasch, Yinfei Yang, and Zhe Gan. Mia-  
 637 bench: Towards better instruction following evaluation of multimodal llms. *arXiv preprint  
 638 arXiv:2407.01509*, 2024.

639

640 Alec Radford, Jong Wook Kim, Chris Hallacy, Aditya Ramesh, Gabriel Goh, Sandhini Agarwal,  
 641 Girish Sastry, Amanda Askell, Pamela Mishkin, Jack Clark, et al. Learning transferable visual  
 642 models from natural language supervision. In *International conference on machine learning*, pp.  
 8748–8763. PMLR, 2021.

643

644 Yuzhang Shang, Mu Cai, Bingxin Xu, Yong Jae Lee, and Yan Yan. Llava-prumerge: Adaptive token  
 645 reduction for efficient large multimodal models. *arXiv preprint arXiv:2403.15388*, 2024.

646

647 Hugo Touvron, Louis Martin, Kevin Stone, Peter Albert, Amjad Almahairi, Yasmine Babaei, Niko-  
 lay Bashlykov, Soumya Batra, Prajjwal Bhargava, Shruti Bhosale, et al. Llama 2: Open founda-  
 tion and fine-tuned chat models. *arXiv preprint arXiv:2307.09288*, 2023.

648 Pavan Kumar Anasosalu Vasu, Fartash Faghri, Chun-Liang Li, Cem Koc, Nate True, Albert Antony,  
 649 Gokul Santhanam, James Gabriel, Peter Grasch, Oncel Tuzel, and Hadi Pouransari. Fastvlm:  
 650 Efficient vision encoding for vision language models, 2025. URL <https://arxiv.org/abs/2412.13303>.  
 651

652 Ke Wang, Junting Pan, Weikang Shi, Zimu Lu, Houxing Ren, Aojun Zhou, Mingjie Zhan, and Hong-  
 653 sheng Li. Measuring multimodal mathematical reasoning with math-vision dataset. *Advances in  
 654 Neural Information Processing Systems*, 37:95095–95169, 2025.

655

656 Zichen Wen, Yifeng Gao, Weijia Li, Conghui He, and Linfeng Zhang. Token pruning in multimodal  
 657 large language models: Are we solving the right problem? *arXiv preprint arXiv:2502.11501*,  
 658 2025a.

659

660 Zichen Wen, Yifeng Gao, Shaobo Wang, Junyuan Zhang, Qintong Zhang, Weijia Li, Conghui He,  
 661 and Linfeng Zhang. Stop looking for important tokens in multimodal language models: Dupli-  
 662 cation matters more, 2025b. URL <https://arxiv.org/abs/2502.11494>.

663

664 Long Xing, Qidong Huang, Xiaoyi Dong, Jiajie Lu, Pan Zhang, Yuhang Zang, Yuhang Cao, Conghui  
 665 He, Jiaqi Wang, Feng Wu, et al. Pyramiddrop: Accelerating your large vision-language models  
 666 via pyramid visual redundancy reduction. *arXiv preprint arXiv:2410.17247*, 2024.

667

668 An Yang, Baosong Yang, Beichen Zhang, Binyuan Hui, Bo Zheng, Bowen Yu, Chengyuan Li,  
 669 Dayiheng Liu, Fei Huang, Haoran Wei, et al. Qwen2.5 technical report. *arXiv preprint  
 670 arXiv:2412.15115*, 2024.

671

672 Weihsao Ye, Qiong Wu, Wenhao Lin, and Yiyi Zhou. Fit and prune: Fast and training-free visual  
 673 token pruning for multi-modal large language models. *Proceedings of the AAAI Conference on  
 674 Artificial Intelligence*, 39(21):22128–22136, Apr. 2025. doi: 10.1609/aaai.v39i21.34366. URL  
<https://ojs.aaai.org/index.php/AAAI/article/view/34366>.

675

676 Jiahui Yu, Zirui Wang, Vijay Vasudevan, Legg Yeung, Mojtaba Seyedhosseini, and Yonghui  
 677 Wu. Coca: Contrastive captioners are image-text foundation models. *arXiv preprint  
 678 arXiv:2205.01917*, 2022.

679

680 Kaichen Zhang, Bo Li, Peiyuan Zhang, Fanyi Pu, Joshua Adrian Cahyono, Kairui Hu, Shuai Liu,  
 681 Yuanhan Zhang, Jingkang Yang, Chunyuan Li, et al. Lmms-eval: Reality check on the evaluation  
 682 of large multimodal models. *arXiv preprint arXiv:2407.12772*, 2024.

683

684 Weichen Zhang, Zhui Zhu, Ningbo Li, Kebin Liu, and Yunhao Liu. Adaptinfer: Adaptive to-  
 685 ken pruning for vision-language model inference with dynamical text guidance. *arXiv preprint  
 686 arXiv:2508.06084*, 2025a.

687

688 Yuan Zhang, Chun-Kai Fan, Junpeng Ma, Wenzhao Zheng, Tao Huang, Kuan Cheng, Denis A Gu-  
 689 dovskiy, Tomoyuki Okuno, Yohei Nakata, Kurt Keutzer, and Shanghang Zhang. SparseVLM:  
 690 Visual token sparsification for efficient vision-language model inference. In *Forty-second In-  
 691 ternational Conference on Machine Learning*, 2025b. URL <https://openreview.net/forum?id=80faIPZ67S>.

692

693 Jinguo Zhu, Weiyun Wang, Zhe Chen, Zhaoyang Liu, Shenglong Ye, Lixin Gu, Yuchen Duan, Hao  
 694 Tian, Weijie Su, Jie Shao, et al. Internvl3: Exploring advanced training and test-time recipes for  
 695 open-source multimodal models. *arXiv preprint arXiv:2504.10479*, 2025.

696

697

698

699

700 Xin Zou, Di Lu, Yizhou Wang, Yibo Yan, Yuanhuiyi Lyu, Xu Zheng, Linfeng Zhang, and Xuming  
 701 Hu. Don't just chase" highlighted tokens" in mllms: Revisiting visual holistic context retention.  
*arXiv preprint arXiv:2510.02912*, 2025.

## 702 A THE USE OF LARGE LANGUAGE MODELS

704 Large language models (LLMs) have increasingly become valuable tools for academic writing and  
 705 manuscript preparation. In this work, we leverage LLMs primarily for **text refinement, language**  
 706 **polishing, and structural editing** of our paper. This includes improving clarity, correcting gram-  
 707 matical errors, rephrasing sentences for conciseness, and ensuring logical flow across sections. Im-  
 708 portantly, LLMs are used only as assistive tools. All scientific content, experiments, and analyses are  
 709 independently designed, implemented, and verified by the authors. We emphasize that LLMs do not  
 710 contribute to the experimental results, numerical analyses, or core intellectual content of this work.  
 711 This responsible usage ensures the integrity and reproducibility of our research while benefiting  
 712 from advanced language capabilities to improve presentation quality.

## 713 B MORE IMPLEMENTATION DETAILS

714 **System Configuration** Our codebase was implemented in Python 3.12 with PyTorch 2.5.1, Trans-  
 715 formers 4.54.0 and CUDA 12.4. All experiments were conducted on NVIDIA A100-40 GB GPUs.

716 **Model Configuration** We evaluate three representative LMM families: LLaVA-v1.5 (7B),  
 717 Qwen2.5-VL (3B & 7B), and InternVL-3 (1B & 8B), all in their official HuggingFace checkpoints  
 718 without fine-tuning or weight modification. For Qwen2.5-VL, we adopt the image pre-processing  
 719 setting `min_pixels=256×28×28` and `max_pixels=1280×28×28`. These settings help the  
 720 model maintain image quality while controlling computational cost and resource consumption.

721 **Method Implementation** Pre-LLM pruning is inserted immediately after the ViT forward: visual  
 722 features are collected, scored by the selected algorithm (Random-Pre, GPrune, DivPrune, etc. ), and  
 723 the kept indices are used to rebuild a shorter multimodal embedding tensor before the LLM sees  
 724 any tokens. Intra-LLM pruning is implemented as a per-layer hook that activates at layer  $K = 2$ ;  
 725 hidden states are split into system, visual and instruction segments, the visual subset is pruned, and  
 726 `position_ids`, `position_embeddings`, and the causal mask are truncated to match the reduced token  
 727 count; the subsequent layer thus computes keys/values only for the kept subset. Attention weights  
 728 required by attention-based methods are obtained with a single eager-mode forward pass, saved to  
 729 a temporary file, and loaded by the prune routine, keeping the modification orthogonal to Flash-  
 730 Attention or SDPA code paths. All pruning decisions are executed after vision encoding and before  
 731 KV-cache construction, ensuring that generation length and memory footprint shrink proportionally.

732 **Metric Calculation** Task scores are produced by the official VLMEvalKit evaluation scripts. For  
 733 MME, we normalise the original counts to a 0–100 scale to align with other datasets; higher values  
 734 indicate better performance. We further compute relative performance, allowing direct comparison  
 735 of accuracy retention across tasks and pruning strengths.

736 **Time Measurement** Wall-clock latency is decomposed into three nested intervals: (1) *total*—end-  
 737 to-end elapsed time for completing the entire benchmark; (2) *prefill*—the compute-bound encoder  
 738 forward pass that processes all visual and textual tokens before the first decode step; (3) *method*—the  
 739 GPU milliseconds consumed inside prefill by the pruning subroutine (token scoring, selection and  
 740 tensor re-layout). Intervals are recorded with on an A100-40 GB, batch size = 1, and averaged over  
 741 three runs.

## 744 C MORE RESULTS

745 We benchmark the pruning performance of existing methods on InternVL3-1B and Qwen2.5-VL-  
 746 3B, with results summarized in Table 6 and Table 7, respectively. Across both model families, we  
 747 observe consistent trends that align with the broader empirical patterns reported in Section Experi-  
 748 ments. These findings reinforce the generality of our benchmark conclusions, indicating that the  
 749 relative strengths and limitations of current pruning techniques are largely preserved across archi-  
 750 tectures of varying scales and designs. Such consistency underscores the reliability of our evaluation  
 751 protocol and highlights the transferable insights that can be drawn from the benchmark results. [Figure 4 visualizes qualitative results of token-retention mask overlays on LLaVA-v1.5-7B and LLaVA-v1.5-13B.](#)

752  
 753  
 754  
 755 xcolor

Table 6: Performance comparison across different methods and benchmarks on InternVL3-1B.

Methods	Comprehensive		OCR	Multidisciplinary		Hallucination		Mathematical		Instruction	Avg.
	MME	MMB-en	SEED	Science QA	POPE	Hallus	Math-V	MathVista	MIA		
<b>InternVL3-1B</b>		<i>Upper Bound, 100% Tokens (100%)</i>									
Vanilla	68.41	73.25	58.41	91.57	89.57	36.13	46.20	18.75	63.48	60.64	
<i>Retain Averaged 33.3% Tokens (↓ 66.7%)</i>											
<b>Random-Pre</b>	65.06	65.45	47.30	83.14	87.39	32.11	37.40	14.14	59.85	54.65	
	↓4.9%	↓10.6%	↓19.0%	↓9.2%	↓2.4%	↓11.1%	↓19.0%	↓24.6%	↓5.7%		
<b>Random-Intra</b>	62.66	35.24	52.14	87.12	87.09	35.33	37.00	16.78	41.88	50.58	
	↓8.4%	↓51.9%	↓10.7%	↓4.9%	↓2.8%	↓2.2%	↓19.9%	↓10.5%	↓34.0%		
<b>FastV</b>	66.52	34.20	45.19	88.65	88.67	34.04	30.50	13.49	38.98	48.91	
	↓2.8%	↓53.3%	↓22.6%	↓3.2%	↓1.0%	↓5.8%	↓34.0%	↓28.1%	↓38.6%		
<b>GPrune</b>	<b>65.78</b>	71.77	49.56	<b>89.74</b>	<b>88.27</b>	<b>33.93</b>	40.80	<b>18.42</b>	<b>62.71</b>	<b>57.89</b>	
	↓3.8%	↓2.0%	↓15.1%	↓2.0%	↓1.4%	↓6.1%	↓11.7%	↓1.8%	↓1.2%		
<b>DivPrune</b>	66.71	<b>71.26</b>	<b>52.61</b>	88.00	88.36	33.13	<b>42.20</b>	14.14	61.38	57.53	
	↓2.5%	↓2.7%	↓9.9%	↓3.9%	↓1.3%	↓8.3%	↓8.7%	↓24.6%	↓3.3%		
<i>Retain Averaged 22.2% Tokens (↓ 77.8%)</i>											
<b>Random-Pre</b>	55.84	63.20	44.93	81.61	85.60	26.61	35.70	14.14	60.70	52.04	
	↓18.4%	↓13.7%	↓23.1%	↓10.9%	↓4.4%	↓26.4%	↓22.7%	↓24.6%	↓4.4%		
<b>Random-Intra</b>	59.41	27.45	43.72	82.42	86.12	33.55	32.40	<b>16.78</b>	46.67	47.62	
	↓13.2%	↓62.5%	↓25.1%	↓10.0%	↓3.8%	↓7.1%	↓29.9%	↓10.5%	↓26.5%		
<b>FastV</b>	64.55	24.24	42.15	85.73	87.55	<b>34.40</b>	31.50	13.49	41.21	47.20	
	↓5.6%	↓66.9%	↓27.8%	↓6.4%	↓2.2%	↓4.8%	↓31.8%	↓28.1%	↓35.1%		
<b>GPrune</b>	56.09	71.08	46.60	<b>88.35</b>	85.43	28.54	<b>38.10</b>	13.16	61.34	54.30	
	↓18.0%	↓3.0%	↓20.2%	↓3.5%	↓4.6%	↓21.0%	↓17.5%	↓29.8%	↓3.4%		
<b>DivPrune</b>	<b>56.93</b>	<b>70.13</b>	<b>49.28</b>	86.66	<b>87.63</b>	28.77	37.90	14.80	<b>63.68</b>	<b>55.09</b>	
	↓16.8%	↓4.2%	↓15.6%	↓5.4%	↓2.1%	↓20.4%	↓17.9%	↓21.1%	↑0.3%		
<i>Retain Averaged 11.1% Tokens (↓ 88.9%)</i>											
<b>Random-Pre</b>	52.63	58.70	41.46	79.52	82.51	25.79	33.20	15.46	<b>61.12</b>	50.04	
	↓23.1%	↓19.8%	↓29.0%	↓13.1%	↓7.8%	↓28.6%	↓28.1%	↓17.5%	↓3.7%		
<b>Random-Intra</b>	55.11	17.06	39.87	80.97	80.65	29.11	29.30	17.76	42.61	43.60	
	↓19.5%	↓76.7%	↓31.7%	↓11.6%	↓9.9%	↓19.4%	↓36.6%	↓5.3%	↓32.8%		
<b>FastV</b>	<b>59.33</b>	19.74	38.46	<b>84.42</b>	82.84	<b>31.90</b>	31.60	18.09	39.26	45.07	
	↓13.3%	↓73.0%	↓34.1%	↓7.8%	↓7.5%	↓11.7%	↓31.6%	↓3.5%	↓38.1%		
<b>GPrune</b>	55.18	<b>66.32</b>	42.95	83.74	75.56	27.09	<b>33.70</b>	11.51	61.84	50.88	
	↓19.4%	↓9.5%	↓26.4%	↓8.5%	↓15.6%	↓25.0%	↓27.1%	↓38.6%	↓2.5%		
<b>DivPrune</b>	55.41	65.80	<b>44.53</b>	83.39	<b>84.58</b>	26.72	<b>36.30</b>	11.84	60.68	<b>52.14</b>	
	↓19.0%	↓10.2%	↓23.8%	↓8.9%	↓5.6%	↓26.0%	↓21.4%	↓36.8%	↓4.4%		

## Deeper Mechanistic Analysis of Visual Token Pruning

This section provides a deeper mechanistic analysis to complement the empirical findings of UNIPRUNEBENCH, addressing the underlying reasons for the observed performance differences across various pruning strategies, task types, and model architectures.

### The Role of Token Redundancy and Random Pruning Effectiveness

The empirical success of random pruning, particularly in general perception tasks, primarily stems from the **high inherent redundancy of visual tokens** generated by Vision Transformers (ViTs) and the sparse reliance of Large Multimodal Models (LMMs) on visual evidence.

- High Redundancy:** For many general understanding tasks, the LMM only requires a small, high-quality subset of visual features. The majority of tokens are redundant. Randomly dropping a large percentage of these tokens often preserves enough semantic structure for robust model function.
- Task Dependence:** This phenomenon is **strictly task-dependent**. On fine-grained tasks such as OCR or mathematical expression parsing, where **precise spatial structure and**

Table 7: Performance comparison across different methods and benchmarks on Qwen2.5-VL-3B.

Methods	Comprehensive		OCR		Multidisciplinary		Hallucination		Mathematical		Instruction	Avg.
	MME	MMB-en	SEED	OCR-B	Science QA	POPE	Hallus	Math-V	MathVista	MIA		
<b>Qwen2.5-VL-3B</b>												
Vanilla	77.0	79.2	68.0	82.3	81.0	86.7	45.3	9.9	38.5	73.5	64.1	
<i>Retain Averaged 33.3% Tokens (↓ 66.7%)</i>												
<b>GPrune</b>	70.6	72.1	59.0	54.6	80.0	83.7	37.8	9.4	34.9	73.0	57.5	
<b>Random-Intra</b>	70.3	73.5	56.0	55.5	80.0	84.3	36.7	9.0	37.5	72.9	57.6	
<b>Random-Pre</b>	72.3	71.7	57.0	55.0	79.0	83.6	35.6	9.6	37.5	72.2	57.4	
<b>DART</b>	72.0	75.6	53.0	56.0	82.0	80.0	38.1	9.0	38.5	73.5	57.8	
<b>FastV</b>	70.7	75.3	57.0	50.7	80.0	85.4	40.3	9.7	38.6	70.4	57.8	
<b>DivPrune</b>	<b>72.6</b>	<b>75.4</b>	<b>60.0</b>	<b>64.9</b>	<b>80.0</b>	<b>86.4</b>	<b>39.7</b>	9.1	<b>39.7</b>	<b>72.5</b>	<b>60.0</b>	
	<b>↓5.7%</b>	<b>↓4.8%</b>	<b>↓11.8%</b>	<b>↓21.1%</b>		<b>↓1.2%</b>	<b>↓0.4%</b>	<b>↓12.4%</b>	<b>↓8.1%</b>	<b>↑3.1%</b>	<b>↓1.4%</b>	
<i>Retain Averaged 22.2% Tokens (↓ 77.8%)</i>												
<b>GPrune</b>	41.9	64.7	54.0	38.5	78.0	79.1	33.8	<b>9.8</b>	33.8	73.3	50.7	
<b>Random-Intra</b>	<b>↓45.6%</b>	<b>↓18.3%</b>	<b>↓20.6%</b>	<b>↓53.2%</b>	<b>↓3.7%</b>	<b>↓8.7%</b>	<b>↓25.4%</b>	<b>↓1.0%</b>	<b>↓12.2%</b>	<b>↓0.3%</b>		
<b>Random-Pre</b>	65.2	70.3	53.0	43.7	80.0	82.3	36.2	9.0	36.2	72.9	54.9	
<b>DART</b>	69.1	70.2	53.0	44.3	79.0	81.7	33.2	9.6	36.9	72.3	54.9	
<b>FastV</b>	68.9	<b>74.4</b>	50.0	48.3	<b>82.0</b>	76.1	<b>37.2</b>	9.0	38.0	72.6	55.7	
<b>DivPrune</b>	<b>↓10.5%</b>	<b>↓6.1%</b>	<b>↓26.5%</b>	<b>↓41.3%</b>	<b>↓1.2%</b>	<b>↓12.2%</b>	<b>↓17.9%</b>	<b>↓9.1%</b>	<b>↓1.3%</b>	<b>↓1.2%</b>		
	<b>↓11.4%</b>	<b>↓9.7%</b>	<b>↓22.1%</b>	<b>↓55.9%</b>		<b>↓1.2%</b>	<b>↓4.7%</b>	<b>↓16.6%</b>	<b>↓5.1%</b>	<b>↓1.8%</b>	<b>↓2.4%</b>	
	<b>69.3</b>	73.9	<b>57.0</b>	<b>57.5</b>	80.0	<b>85.3</b>	36.9	9.2	<b>39.1</b>	<b>73.9</b>	<b>58.2</b>	
	<b>↓10.0%</b>	<b>↓6.7%</b>	<b>↓16.2%</b>	<b>↓30.1%</b>		<b>↓1.2%</b>	<b>↓1.6%</b>	<b>↓18.5%</b>	<b>↓7.1%</b>	<b>↑1.6%</b>	<b>↑0.5%</b>	
<i>Retain Averaged 11.1% Tokens (↓ 88.9%)</i>												
<b>GPrune</b>	20.6	52.6	49.0	14.5	75.0	68.6	27.9	8.9	27.0	68.3	41.3	
<b>Random-Intra</b>	<b>↓73.2%</b>	<b>↓33.6%</b>	<b>↓27.9%</b>	<b>↓82.4%</b>	<b>↓7.4%</b>	<b>↓20.8%</b>	<b>↓38.4%</b>	<b>↓10.1%</b>	<b>↓29.9%</b>	<b>↓7.1%</b>		
<b>Random-Pre</b>	60.3	65.5	48.0	30.8	77.0	77.2	31.2	8.8	34.8	72.0	50.6	
<b>DART</b>	62.6	65.1	48.0	30.5	77.0	76.0	29.0	9.3	35.5	72.2	50.5	
<b>FastV</b>	62.0	<b>69.9</b>	47.0	29.5	<b>81.0</b>	68.0	<b>33.1</b>	<b>9.7</b>	33.1	73.1	50.6	
<b>DivPrune</b>	<b>↓73.2%</b>	<b>↓28.5%</b>	<b>↓27.9%</b>	<b>↓77.4%</b>	<b>↓2.5%</b>	<b>↓16.8%</b>	<b>↓26.7%</b>	<b>↓9.1%</b>	<b>↓19.0%</b>	<b>↓6.1%</b>		
	<b>63.3</b>	70.2	<b>52.0</b>	<b>43.1</b>	78.0	<b>81.7</b>	34.8	9.0	<b>36.9</b>	<b>75.0</b>	<b>54.4</b>	
	<b>↓17.8%</b>	<b>↓11.4%</b>	<b>↓23.5%</b>	<b>↓47.6%</b>		<b>↓3.7%</b>	<b>↓5.8%</b>	<b>↓23.2%</b>	<b>↓9.1%</b>	<b>↓4.2%</b>	<b>↓2.0%</b>	

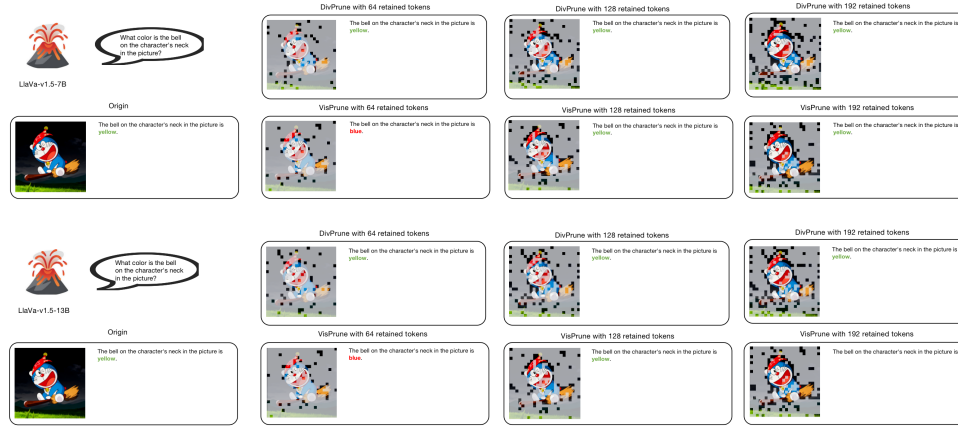


Figure 4: Qualitative results of token-retention mask overlays on LLaVA-1.5-7B and on LLaVA-1.5-13B.

**local visual cues** are critical, random pruning exhibits sharp and consistent degradation. This confirms that random pruning, while effective for coarse redundancy removal, is fundamentally limited for detail-sensitive tasks.

864 D.2 PRUNING STAGE AND INFORMATION FLOW (*ViT*-ONLY VS. *LLM*-ONLY)865  
866 The choice of pruning stage—before or during cross-attention—significantly impacts performance,  
867 explaining why *ViT*-only pruning often outperforms *LLM*-only pruning on certain architectures.  
868869 1. **ViT-only Pruning (Pre-modulation):** Pruning at the raw *ViT* feature stage removes redundancy  
870 while preserving the full **high-fidelity embedding space** before the visual tokens are  
871 modulated by cross-attention. This maintains the fidelity of critical visual information.  
872 2. **LLM-only Pruning (Post-modulation):** Pruning after the *LLM* has processed the visual  
873 tokens may inadvertently remove tokens that have become **query-conditioned or**  
874 **attention-amplified**. If the cross-attention mechanism has not perfectly highlighted all  
875 semantically critical regions, subsequent pruning risks removing complementary tokens,  
876 potentially making the process more harmful.  
877

## 878 D.3 TASK SENSITIVITY AND ROBUSTNESS PROFILES

879 The observed divergent robustness profiles across capability dimensions are directly explained by  
880 the inherent visual dependence and language prior strength of the task.  
881882 1. **Vulnerability (e.g., OCR, Math Parsing):** These tasks depend on **precise local visual**  
883 **cues and fine-grained spatial structures**. Token loss in these areas directly compromises  
884 the required precision, making these tasks highly vulnerable to token pruning.  
885 2. **Robustness (e.g., Instruction-Following):** These tasks are more robust to coarse-grained  
886 visual summaries due to stronger **language priors** and less reliance on token-level spatial  
887 patterns. The *LLM* can often infer the correct response based on the text prompt and a  
888 general understanding of the image.  
889

## 890 D.4 DEEP DIVE INTO METHOD-SPECIFIC BEHAVIOR

891 Different pruning strategies show distinct behavior depending on the pruning ratio  $\rho$  and architec-  
892 tural constraints.  
893894 1. **Importance-Based Methods (e.g., SparseVLM) under Light Pruning ( $1 - \rho \ll 1$ ):** Methods  
895 relying on learned importance estimators (e.g., magnitude scores or attention  
896 strength) excel under light pruning. They effectively remove truly redundant tokens while  
897 retaining all semantically critical regions.  
898 2. **Diversity-Based Methods (e.g., DivPrune) under Heavy Pruning ( $1 - \rho \approx 1$ ):** Diversity-  
899 preserving methods, which focus on maintaining **spatial coverage and feature hetero-**  
900 **geneity**, are more stable under heavy pruning. Importance-score methods risk collapsing  
901 onto a few highly attended regions, losing complementary cues. Diversity-based methods  
902 maintain a **representative global token set**, retaining holistic scene structure and enabling  
903 superior robustness under extreme compression.  
904 3. **Architecture–Method Interactions:** The efficacy is influenced by *LMM* architecture de-  
905 tails, such as fusion depth and attention distribution sharpness. Architectures with sharper  
906 cross-attention distributions benefit more from importance-driven pruning under light com-  
907 pression, while those with dispersed attention may favor diversity-based methods. This  
908 necessitates careful method selection based on the target *LMM* family.  
909  
910  
911  
912  
913  
914  
915  
916  
917